JOURNAL OF AGRICULTURAL AND FOOD CHEMISTRY

Effect of the Molecular Mass and Degree of Substitution of Oleoylchitosan on the Structure, Rheological Properties, and Formation of Nanoparticles

YAN YAN LI,† XI GUANG CHEN,*,† CHENG SHENG LIU,† DONG SU CHA,§ HYUN JIN PARK,§ AND CHONG M. LEE#

College of Marine Life Science, Ocean University of China, 5 Yu Shan Road, Qingdao 266003, People's Republic of China; Graduate School of Biotechnology, Korea University, 1 5-Ka, Anam-Dong, Sungbuk-Ku, Seoul 136-701, South Korea; and Department of Food Science and Untrition, University of Rhode Island, Kingston, Rhode Island 02881

Oleoylchitosans (O-chitosans), with different molecular masses and degrees of substitution (DS), were synthesized by reacting chitosan with oleoyl chloride. The FT-IR suggested the formation of an amide linkage between amino groups of chitosan and carboxyl groups of oleic acid. The viscosity of O-chitosan sharply increased with the increase of concentration, whereas that of unmodified chitosan rose only slightly. This increase was stronger as the increase of hydrophobicity (DS) and molecular mass of the polymer. The critical aggregation concentration (CAC) of O-chitosans with DS 5, 11, and 27% were 79.43, 31.6, 10 mg/L, respectively, and the CAC of samples with molecular masses of 20, 38, 300, and 1100 kDa were 50.1, 74.93, 125.9, and 630.9 mg/L, respectively. All of the O-chitosans could reduce surface tension slightly. Nanoparticles were prepared using an O/W emulsification method. Mean diameters of the polymeric amphiphilic nanoparticles of O-chitosans with DS 5 and 11% were around 327.4 and 275.3 nm, respectively.

KEYWORDS: O-chitosan; viscosity; surface tension; fluorescence; nanoparticles

INTRODUCTION

Amphiphilic copolymers consisting of hydrophilic and hydrophobic segments can form micelle structures with the hydrophobic inner core and the hydrophilic outer shell in aqueous media. The hydrophobic inner core is surrounded by a hydrophilic outer shell, which provides a stabilizing interface between the micelle core and the aqueous environment (*1*, *2*). These polymeric nanoparticles exhibit unique characteristics, depending on their hydrophobic/hydrophilic constituents, such as unusual rheological features, a nanoscale hydrodynamic radius with core−shell structure, and thermodynamic stability (*3*, *4*). Polymeric micelles have received special attention due to their potential application and academic interest in many interdisciplinary fields (*5*, *6*). Because the hydrophobic core and hydrophilic shell need to be biodegradable and nontoxic, many investigations of hydrophobic polymers are focused on natural biomaterials.

Chitosan, *R*-(*1*−*4*)-2-amino-2-deoxy-α-D-glucan, is a partially deacetylated form of chitin, an abundant natural polysaccharide present in crustacean shells. Its unique characteristics such as positive charge, biodegradability, biocompatibility, nontoxicity, and rigid linear molecular structure make this macromolecule ideal as a drug carrier and delivery material (*7*, *8*). There have been many reports of hydrophobic modifications of chitosan and nanoparticle formation by self-aggregation in aqueous solution (*9*, *10*). These modifications can introduce hydrophobic groups into chitosan and produced chitosan amphiphilic polymers. Some of these chitosan amphiphilic derivatives can form nanosized self-aggregation in aqueous media (*11*). Long-chain fatty acyl derivatives of chitosan are novel hydrophobic modifications that can form nanoparticles. Few studies on the effect of structure of the chitosan amphiphilic derivatives on the formation of nanoparticles have been carried out. Moreover, through adjusting the structure of the amphiphilic copolymers (the molecular weight and the ratio of hydrophobic group to hydrophilic group) (*12*), the size and morphology of the polymeric micelles may be easily controlled.

In this paper, oleoylchitosans (O-chitosans) with different molecular masses and degrees of substitution (DS) were prepared. The molecular structures of O-chitosans were analyzed by FT-IR. The effects of molecular mass and DS of O-chitosan on the structure, rheological properties, and formation of nanoparticles were measured by viscosity, surface tension, and fluorescence methods. Nanoparticles were prepared using an O/W emulsification method. The morphology and size of nanoparticles were measured by transmission electron microscopy (TEM) and dynamic light scattering (DLS).

* Author to whom correspondence should be addressed (telephone 86-0532-82032586; fax 86-0532-82032586; e-mail xgchen@ouc.edu.cn).
† Ocean University of China.
§ Korea University.
# University of Rhode Island.

10.1021/jf062648m CCC: $37.00
Published on Web 05/11/2007

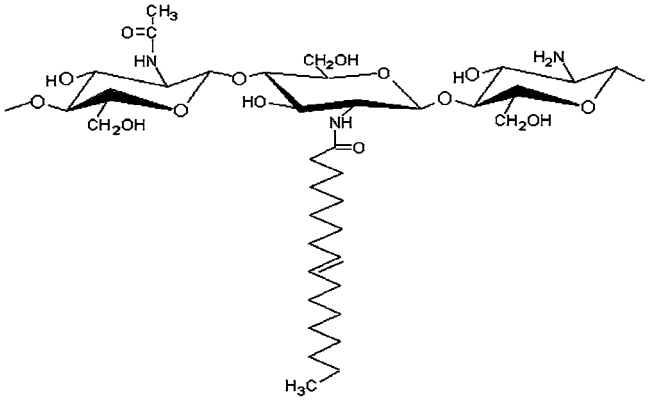

Figure 1. Chemical structure of oleoylchitosan (O-chitosan).

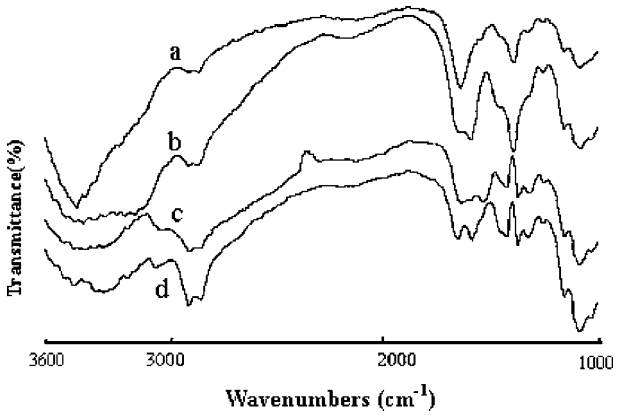

Figure 2. FT-IR of chitosan and O-chitosans with different DS: (**a**) chitosan (mol mass = 38 kDa); (**b**) O-chitosan (DS 5%); (**c**) O-chitosan (DS 11%); (**d**) O-chitosan (DS 27%).

Table 1. Oleoylchitosan Samples with Different Degrees of Substitution (DS) and Molecular Masses

series	sample	DS (%)	mol mass (kDa)
1	1	5	20
	2	5	38
	3	5	300
	4	5	1100
2	2	5	38
	5	11	38
	6	27	38

MATERIALS AND METHODS

Materials. Chitin, degree of deacetylation = 82% and molecular mass = 1100 kDa, was made from crab shell and obtained from Biotech Co. Pyrene, oleoyl chloride, pyridine, chloroform, methylene chloride, ethanol, acetic acid, and sodium tripolyphosphate (STPP) were purchased from Sigma Chemicals and used without further purification.

Preparation and Characterization of O-chitosan. Chitosan was degraded by the method of acetic acid hydrolysis, and viscosity molecular mass was calculated by using an Ubbelohde Viscosimeter referenced from Chen (*13*). Different molecular mass chitosan samples are shown in **Table 1**. O-chitosan was prepared by reacting chitosan with oleoyl chloride referenced from Zong (*14*). The O-chitosans with different DS were prepared by controlling the feed ratio of chitosan to oleoyl chloride. O-chitosans with different molecular masses were prepared using the chitosans of different molecular masses. The degree of N-acylation, which can be defined as the number of oleic acid groups per 100 anhydroglucose units of chitosan, was evaluated according to an FT-IR method (*15*).

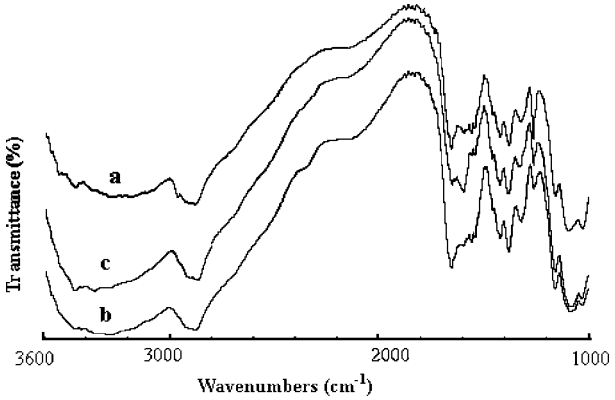

Figure 3. FT-IR of O-chitosans with different molecular masses: (**a**) 1100 kDa; (**b**) 300 kDa; (**c**) 38 kDa.

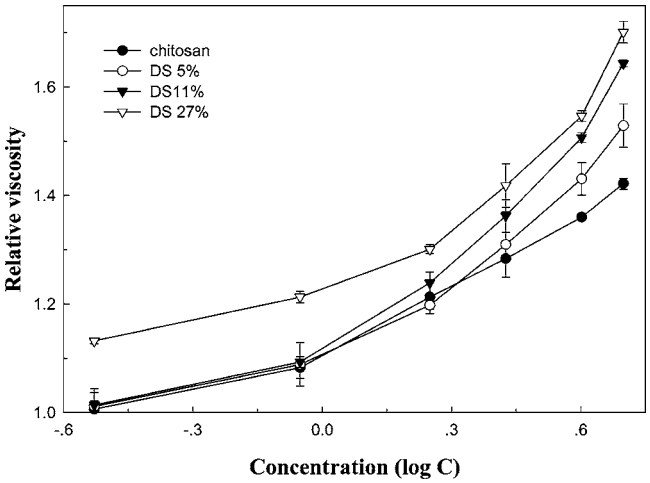

Figure 4. Viscosity of chitosan and O-chitosans with different DS.

The FT-IR spectra of chitosan and O-chitosan were recorded on an Avater-360 Fourier transform infrared spectrometer (Nicolet) at 20 °C following the method of Shigemasa et al. (*16*). For the IR spectroscopic analysis, 2 mg of the samples was mixed with 100 mg of KBr and made into pellets.

Rheology Behavior of O-chitosan. The rheological measurements were carried out with an Ubbelohde viscometer with a capillary diameter of 0.55 mm, within the range of polymer concentration from 0.3 to 5.0 g/L (*17*). Relative viscosity (η_r) is the ratio of the time of the solution to that of the pure solvent ($\eta_r = t/t_0$, where t is the flow time of the solution and t_0 is the flow time of the solvent). The variation of the relative viscosity with polymer concentration is presented in **Figures 4** and **5**.

Surface Tension Measurement. The aggregation behavior of the O-chitosan at the air−water interface was determined by the measurements of surface tension. The surface tension measurements of chitosan and O-chitosan solutions at various concentrations were carried out on a Krüss K12 Processor Tensionmeter with the plate method of Wilbelmy at 30 ± 0.1 °C. All of the solutions were kept at room temperature for 1 day before surface tension measurement (*18*).

Measurement of Fluorescence Spectroscopy. Pyrene, used as a hydrophobic probe, was used at the final concentration was 2 μM. The mixture was incubated for 3 h in a water bath at 65 °C and shaken in a BS-10 shaking water bath overnight at 20 °C. Pyrene emission spectra were obtained using a Shimadzu RF-5301PC fluorescence spectrophotometer. The probe was excited at 343 nm, and the emission spectrum was collected in the range of 360−500 nm at an integration time of 1.0 s. The excitation and emission slit openings were 15 and 1.5 nm, respectively.

Preparation of Self-Aggregation Nanoparticles. Thirty milligrams of O-chitosan was dissolved in 10 mL of 0.1 M acetic acid solution. Methylene chloride (3%, v/v) was added to the O-chitosan acetic acid

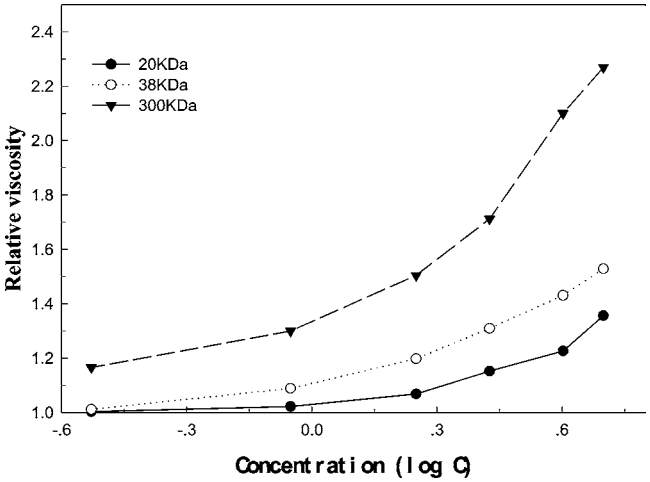

Figure 5. Viscosity of O-chitosans with different molecular masses.

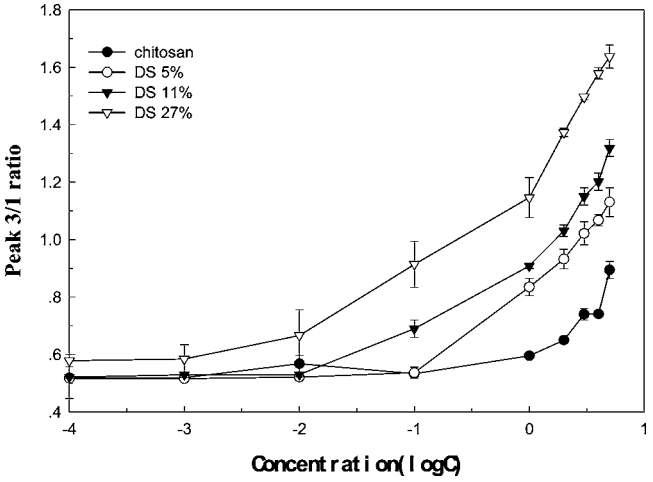

Figure 6. Peak I_3/I_1 ratio of pyrene fluorescence as a function of O-chitosans with different DS in 1% (v/v) acetic acid.

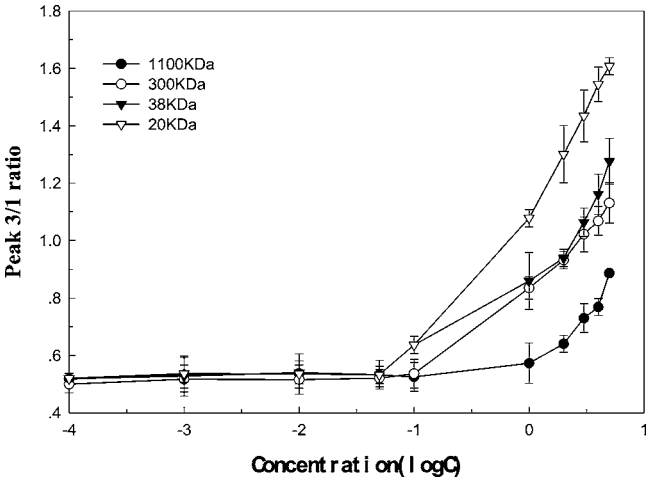

Figure 7. Peak I_3/I_1 ratio of pyrene fluorescence as a function of O-chitosans with different molecular masses in 1% (v/v) acetic acid.

Table 2. Surface Tension of Oleoylchitosans[a]

		surface tension (mN/m)		
series	sample	1 g/L	5 g/L	10 g/L
1	2	71.10 ± 0.01	68.35 ± 0.01	67.19 ± 0.03
	3	71.30 ± 0.02	68.45 ± 0.01	67.09 ± 0.08
	4	71.50 ± 0.04	68.64 ± 0.06	67.2 ± 0.06
2	chitosan	71.60 ± 0.02	68.53 ± 0.03	67.23 ± 0.01
	2	71.10 ± 0.01	68.35 ± 0.01	67.19 ± 0.03
	5	69.10 ± 0.02	66.38 ± 0.04	64.4 ± 0.02
	6	67.10 ± 0.05	61.34 ± 0.02	61.01 ± 0.03

[a] Values are means ± standard deviation ($n = 3$).

solution with stirring and homogenized (5 min, 13000*g*) with an Ultra-Turrax T-25 dispersing machine. Methylene chloride was chosen because of its ability to diffuse into the aqueous phase at a rapid rate, facilitating particle formation upon evaporation. The solution was held under vacuum for 30 min at 20 °C to remove methylene chloride, and then 1 mL of 0.25% STPP solution was added as a cross-linking reagent (*19*).

Transmission Electron Microscopy. The morphology of the nanoparticles was observed by TEM with a JEM-2010. Solution of O-chitosans were placed onto a copper grill covered with nitrocellulose. They were dried at room temperature and then were examined using TEM by negative staining with an aqueous solution of sodium phosphotungstate.

Determination of Nanoparticle Size. The size distribution of nanoparticles were measured by DLS with a Zetasizer 3000. All DLS measurements were done with a wavelength of 632.8 nm at 23 °C.

Statistical Analyses. The assays were performed at least in triplicate on separate occasions. The data collected in this study are expressed as the mean value ± standard deviation.

RESULTS AND DISCUSSION

Preparation and Characterization of O-chitosan. The O-chitosans with different DS and molecular masses are shown in **Table 1**. The structure of O-chitosan is shown in **Figure 1**.

The infrared spectra of chitosan and O-chitosan with different DS are shown in **Figure 2**. Compared to the IR spectrum of chitosan, the spectra of O-chitosan exhibited many alterations: The absorption at 3000−3600 cm^{-1} (OH, NH_2) decreased, and the band at 1570 cm^{-1} (δ N−H of amide) decreased, whereas prominent bands at 1655 cm^{-1} (ν C═O) and 1555 cm^{-1} (δ N−H of amide II) were observed. The peaks at 2924 cm^{-1} (ν_{as} CH_2), 2854 cm^{-1} (ν_s CH_2), 1464 cm^{-1} (δ CH_2), and 1182 cm^{-1} (twisting vibration of CH_2) were stronger and sharper in the high DS sample, and their intensity was proportional to the DS value. These results confirmed that the chitosan was substituted with oleoyl (*20*).

The infrared spectra of O-chitosans having different molecular masses (38, 300, and 1100 kDa) are shown in **Figure 3**. All of the spectra of different molecular mass O-chitosans had similar profiles, which was consistent with an earlier study that the spectra of different molecular mass chitosans had no obvious differences (*21*). The results showed that O-chitosan samples made from the method we used had no obvious change in molecular structure.

Rheology Behavior of O-chitosan. The relative viscosity of O-chitosans with different DS (5, 11, and 27%) in 0.2 M HCl is shown in **Figure 4**. The viscosity of O-chitosan was always somewhat higher than that of unmodified chitosan. The viscosity of O-chitosan sharply increased with the increase of concentration, whereas that of unmodified chitosan rose only slightly. This increase was stronger as the DS increased. Moreover, the concentration at which this increase was marked compared with the chitosan curve decreased when the DS increased. This was due to the presence of interactions between polymer chains. The formation of hydrophobic domains detected on a molecular level was accompanied by an increase of the viscosity of aqueous solutions of polymer. An association process leading to the formation of bridges between neighboring flower aggregates occurred as the polymer concentration increased (*22*, *23*). A

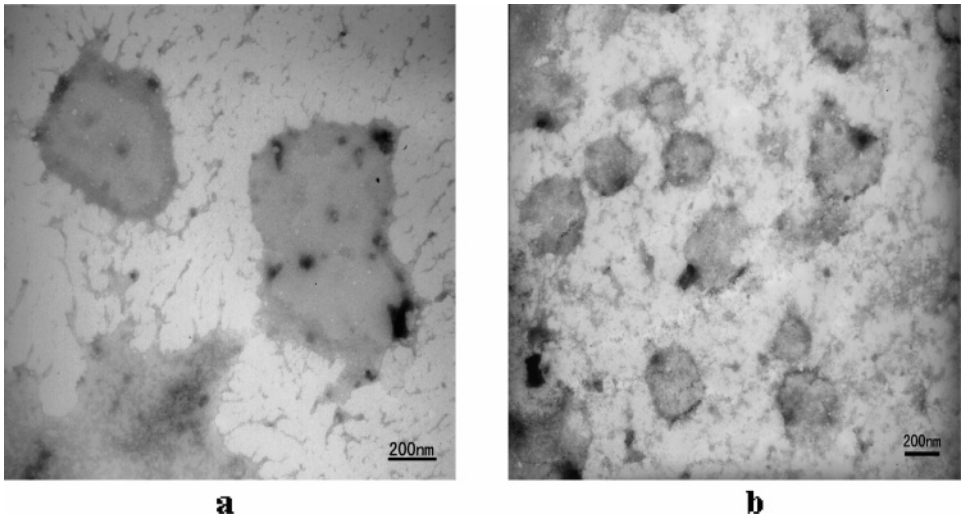

Figure 8. Transmission electron microscopy photographs of O-chitosan nanoparticles with different DS: (**a**) DS 5% (30000×); (**b**) DS 11% (25000×).

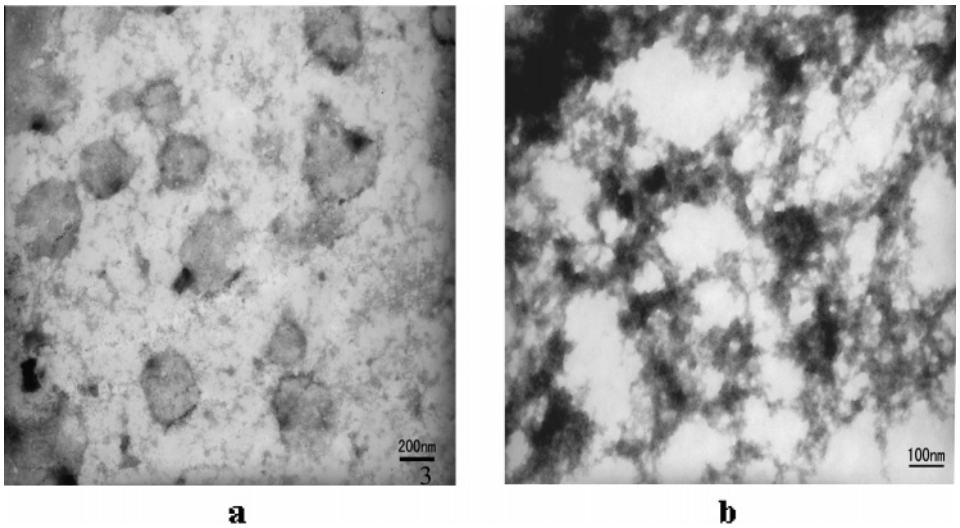

Figure 9. Transmission electron microscopy photographs of O-chitosan nanoparticles with different molecular masses: (**a**) 1100 kDa (25000×); (**b**) 38 kDa (50000×).

connecting network was then formed from the percolation of bridges leading to a large increase in the solution viscosity. Hence, we could suggest that these hydrophobic domains played the role of junction zones, which linked multiple polymer molecules together in an intermolecular aggregate. Therefore, O-chitosan demonstrated a behavior typical of many associating polyelectrolytes.

The relative viscosity of different molecular mass (20, 38, and 300 kDa) O-chitosans is shown in **Figure 5**. The viscosity rose with the increase of polymer concentration, particularly for high molecular mass samples. The viscosity of high molecular mass O-chitosan was greater than that of the low molecular mass one. The trend was similar to the chitosans with different molecular masses (*24*). Although there were interactions between polymer chains, hydrogen bonds, electrostatic bonds, and hydrophobic interactions, the molecular mass was the main factor that affected the viscosity of O-chitosan. There were more entangled junctions in solution of high molecular mass samples, and the chains of high molecular mass O-chitosans were less flexible than those of lower molecular mass ones.

Surface Tension of O-chitosan. Due to their amphiphilic structure, O-chitosans also had potential surface and interfacial properties. O-chitosan was dissolved in 0.1 M acetic acid solution for surface tension measurements. The surface tensions of O-chitosans with different DS (5, 11, and 27%) are shown in **Table 2**. It was shown that the surface tension of O-chitosan decreased with the increase of DS. The surface tensions of samples of 10 g/L with DS 5, 11, and 27% were 67.19 ± 0.05, 64.4 ± 0.02, and 61.01 ± 0.03 mN/m, respectively. More amphiphilic polymers got to the surface of the solution with the increase of DS of the hydrophobic groups, so the ability to decrease the surface tension improved. These phenomena were confirmed by the fluorescence measurement. The product with high DS had more hydrophobic groups and might have more possibility to adsorb alkyl side chains, forming dense packing at the interface. The stiffness of the backbones and the charge density for polyelectrolytes of O-chitosans also affected the adsorption at the air−water interface.

The surface tensions of O-chitosans with different molecular masses (38, 300, and 1100 kDa) are shown in **Table 2**. It was shown that the surface tensions of different molecular mass O-chitosans are similar, which was inconsistent with an earlier study that in the solution of low molecular mass nonionic type chitosan surfactant, the small space steric and small chain flexibility of the backbones made the microstructure and distribution of hydrophobic groups and hydrophilic groups more balanceable, so the ability to decrease surface tension improved

(*25*). The reason might be that all O-chitosan samples had only a slight ability to decrease the surface tension, so the surface tension of different molecular mass samples had no obvious difference.

These results demonstrated that the introduction of hydrophobic substituents made the resulting derivatives more amphiphilic, which can decrease the surface tension. As the concentration grows, more macromolecules unfold at the interface and might adsorb irreversibly by "anchoring" their multiple hydrophobic functional groups into the nonpolar phase. However, different from low molecule surfactants, the O-chitosan showed only a slight ability to decrease the surface tension (*26*). The reason might be that for the amphiphilic polymer, the hydrophobic chains of different O-chitosan molecules could associate to form aggregation in the solution while they concentrated on the surface before the surface tension reached the lowest value.

Fluorescence Spectroscopy. The semilogarithmic plots of I_3/I_1 (I_{383}/I_{372}) versus concentration of O-chitosans with different DS (5, 11, and 27%) and chitosan are shown in **Figure 6**. The high DS O-chitosan had a more pronounced hydrophobic character than the low DS sample. Poor ability to form micelle aggregates was observed with the low substituted O-chitosan (DS 5%). The critical aggregation concentration (CAC) value determined in acidic aqueous media was 79.43 mg/L. In contrast to this, the CAC values of samples with DS 11 and 27% were 31.6 and 10 mg/L, respectively. Increasing DS (5−27%) resulted in a significant decrease of CAC. A higher degree of hydrophobic substitutions in the macromolecule of O-chitosan might facilitate its self-aggregation, favoring hydrophobic interactions and, thus, the formation of dense polymer aggregates.

The effect of the molecular mass (20, 38, 300, and 1100 kDa) of O-chitosans on the I_3/I_1 ratio is shown in **Figure 7**. It was shown that low molecular mass O-chitosan had a more pronounced hydrophobic character than the high molecular mass sample. Poor ability to form micelle aggregates was observed with the high molecular massMW O-chitosan. The CAC values of samples with molecular masses of 20, 38, 300, and 1100 kDa were 50.1, 74.93, 125.9, and 630.9 mg/L, respectively. For the samples with different molecular masses, although the ratio of hydrophobic group to hydrophilic group was similar, the significant chain stiffness of the backbones and large space steric of high molecular mass samples affected the aggregation properties. It was reported in an earlier study that the I_3/I_1 ratio of high molecular mass chitosan was higher than that of the low molecular mass chitosan reported by Mansoor (*27*). This means that the modification of the long-chain oleoyl group had changed the property of chitosan severely.

TEM of the O-chitosan Nanoparticles. The morphology of O-chitosan nanoparticles was investigated by TEM. The nanoparticles of O-chitosans with different DS are shown in **Figure 8**. Nanoparticles were seen in samples with DS 5 and 11%, whereas they were not seen in the DS 27% sample. The polymeric nanoparticles were nearly spherical in shape. In the high DS sample, although the increase of DS might facilitate its self-aggregation, which we had concluded from the result of fluorescence spectroscopy, with high viscosity and low solubility nanoparticles were not readily formed. Hence, we could suggest that the increase of DS might facilitate the formation of nanoparticles, but the DS should be not too large to have a compromise between solubility and viscosity.

The TEM of nanoparticles of O-chitosans with molecular masses of 38 and 1100 kDa is shown in **Figure 9**. Nanoparticles were seen in samples with a molecular mass of 38 kDa, whereas they were not seen in the sample with a molecular mass of 1100 kDa. In the high molecular mass sample, the significant stiffness of the backbones and the high viscosity of the large molecule made it very hard to form nanoparticles. Hence, we could suggest that the decrease of molecular mass might facilitate the formation of nanoparticles.

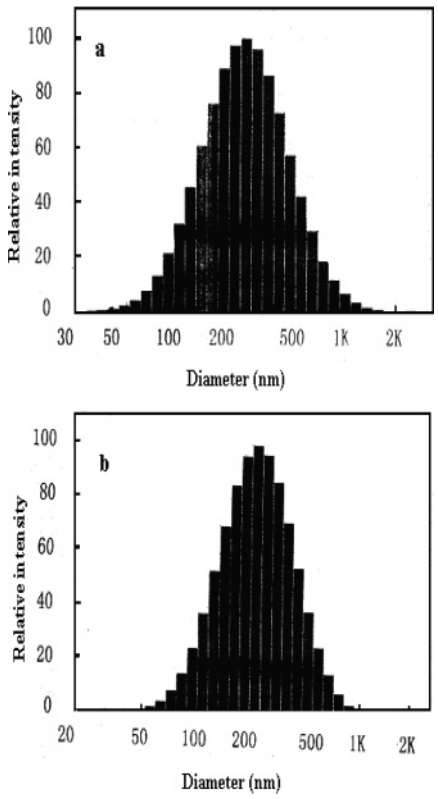

Figure 10. Size distribution of O-chitosan nanoparticles with different DS: (**a**) DS 11%; (**b**) DS 5%.

Size Distribution. From the results, O-chitosans with DS 5 and 11% were selected for further size distribution experiments because of their good shape, low viscosity, and low surface tension in aqueous solution. **Figure 10** shows the size distribution of the nanoparticles formed by O-chitosans with DS 5 and 11% (3 g/L) in the 0.1 M acetic acid solution. The majority of particles were around 327.4 and 275.3 nm in size. The size of self-aggregates decreased as the DS increased, indicating formation of denser hydrophobic cores in high DS sample (*28*). This was consistent with the fluorescence spectroscopy findings.

Form the results of morphology and size distribution, we could suggest that the increase of DS and decrease of molecular mass might facilitate the formation of nanoparticles but that the DS should be not too large to have a compromise between solubility and viscosity.

Nevertheless, these results indicated that O-chitosan had a hydrophobic core inside the self-aggregate, and these hydrophobic cores might be available to load various amphiphilic and hydrophobic drugs into the self-aggregate.

In summary, the structure, rheological properties, and formation of nanoparticles of oleoylchitosans were affected by degree of substitution and molecular mass. The viscosity of O-chitosan sharply increased with the increase of concentration, whereas that of unmodified chitosan rose only slightly. This increase was stronger as the DS and molecular mass of the polymer increased. The increase of DS and decrease of molecular mass resulted in a significant decrease of critical aggregation concentration. All of the O-chitosans could reduce surface tension

slightly. Nanoparticles were prepared using an O/W emulsification method. The mean diameters of the polymeric amphiphilic nanoparticles of O-chitosans with DS 5 and 11% were around 327.4 and 275.3 nm, respectively.

LITERATURE CITED

(1) Janes, K. A.; Calvo, P.; Alonso, M. J. Polysaccharide colloidal particles as delivery systems for macromolecules. *Adv. Drug Delivery Rev.* **2001**, *47*, 83−97.

(2) Kwon, G. S.; Kataoka, K. Block copolymer micelles as long-circulating drug vehicles. *Adv. Drug Delivery Rev.* **1995**, *6*, 295−309.

(3) Kakizawa, Y.; Harada, A.; Kataoka, K. Glutathione-sensitive stabilization of block copolymer micelles composed of antisense DNA and thiolated poly(ethylene glycol)-block-poly(L-lysine): a potential carrier for systemic delivery of antisense DNA. *Biomacromolecules* **2001**, *2*, 491−497.

(4) Richards, M. P.; Chaiyasit, W.; McClements, D. J.; Decker, E. A. Ability of surfactant micelles to alter the partitioning of phenolic antioxidants in oil-in-water emulsions. *J. Agric. Food Chem.* **2002**, *50*, 1254−1259.

(5) Nishikawa, T.; Akiyoshi, K.; Sunamoto, J. Supramolecular assembly between nanoparticles of hydrophobized polysaccharide and soluble protein complexation between the self-aggregate of cholesterol-bearing pullulan and α-chymotrypsin. *Macromolecules* **1994**, *27*, 7654−7659.

(6) Zhang, X. C.; Jackson, J. K.; Burt, H. M. Development of amphiphilic diblock copolymers as micellar carriers of taxol. *Int. J Pharm.* **1996**, *132*, 195−206.

(7) Gupta, K. C.; Jabrail, F. H. Glutaraldehyde and glyoxal cross-linked chitosan microspheres for controlled delivery of centchroman. *Carbohydr. Res.* **2006**, *341*, 744−756.

(8) Li, F.; Liu, W. G.; Yao, K. D. Preparation of oxidized glucosecross-linked N-alkylated chitosan membrane and in vitro studies of pH-sensitive drug delivery behaviour. *Biomaterials* **2002**, *23*, 343−347.

(9) Kim, Y. H.; Gihm, S. H.; Park, C. R.; Lee, K. Y.; Kim, T. W.; Kwon, I. C.; Chung, H.; Jeong, S. Y. Structural characteristics of size-controlled self-aggregates of deoxycholic acid-modified chitosan and their application as a DNA delivery carrier. *Bioconjugate Chem.* **2001**, *12*, 932−938.

(10) Liu, C. G.; Desai, K. G.; Chen, X. G.; Park, H. J. Linolenic acid-modified chitosan for formation of self-assembled nanoparticles. *J. Agric. Food Chem.* **2005**, *53*, 437−441.

(11) Janes, K. A.; Fresneau, M. P.; Marazuela, A.; Fabra, A.; Alonso, M. J. Chitosan nanoparticles as delivery systems for doxorubicin. *J. Controlled Release* **2001**, *73*, 255−267.

(12) Kim, K.; Kwon, S.; Park, J. H.; Chung, H.; Jeong, S. Y.; Kwon, I. C.; Kim, I. S. Physicochemical characterizations of self-assembled nanoparticles of glycol chitosan−deoxycholic acid conjugates. *Biomacromolecules* **2005**, *6*, 1154−1158.

(13) Wang, Q. Z.; Chen, X. G.; Liu, N.; Wang, S. X.; Liu, C. S.; Meng, X. H.; Liu, C. G. Protonation constants of chitosan with different molecular weight and degree of deacetylation. *Carbohydr. Polym.* **2006**, *65*, 194−201.

(14) Zong, Z.; Kimura, Y.; Takahashi, M.; Yamane, H. Characterization of chemical and solid state structures of acylated chitosans. *Polymer* **2000**, *41*, 899−906.

(15) Lee, K. Y.; Ha, W. S.; Park, W. H. Blood compatibility and biodegradability of partially N-acylated chitosan derivatives. *Biomaterials* **1995**, *16*, 1211−1216.

(16) Shigemasa, Y.; Matsuura, H.; Sashiwa, H.; Saimoto, H. Evaluation of different absorbance ratios from infrared spectroscopy for analyzing the degree of deacetylation in chitin. *Int. J Biol. Macromol.* **1996**, *18*, 237−242.

(17) Philippova, O. E.; Volkov, E. V.; Sitnikova, N. L.; Khokhlov, A. R.; Desbrieres, J.; Rinaudo, M. Two types of hydrophobic aggregates in aqueous solutions of chitosan and its hydrophobic derivative. *Biomacromolecules* **2001**, *2*, 483−490.

(18) Sui, W. P.; Song, G. L.; Chen, G. H.; Xu, G. Y. Aggregate formation and surface activity property of an amphiphilic derivative of chitosan. *Colloids Surf. A* **2005**, *256*, 29−33.

(19) Chen, X. G.; Lee, C. M.; Park, H. J. O/W Emulsification for the self-aggregation and nanoparticle formation of linoleic acids modified chitosan in the aqueous system. *J. Agric. Food Chem.* **2003**, *51*, 3135−3139.

(20) Le Tien, C.; Lacroix, M.; Ispas-Szabo, P.; Mateescu, M. A. N-acylated chitosan: hydrophobic matrices for controlled drug release. *J. Controlled Release* **2003**, *93*, 1−13.

(21) Qun, G.; Ajun, W. Effects of molecular weight, degree of acetylation and ionic strength on surface tension of chitosan in dilute solution. *Carbohydr. Polym.* **2006**, *64* 29−36.

(22) Le Meins, J. F.; Tassin, J. F. Shear-induced phase separation in an associating polymer solution. *Macromolecules* **2001**, *34*, 2641−2647.

(23) Semenov, A. N. Dynamics of entangled associating polymers with large aggregates. *Macromolecules* **2002**, *35*, 4821−4837.

(24) Lairez, D.; Adam, M.; Carton, J. P.; Raspaud, E. Aggregation of telechelic triblock copolymers: from animals to flowers. *Macromolecules* **1997**, *30*, 6798−680.

(25) Fan, J. S.; Zhang, Q. F.; Xu, G. Y.; Sun, M. K.; Chen, G. J. The influence of molecular weight on the surface activity of non-ionic type chitosan surfactants. *Polym. Mater. Sci. Eng.* **2004**, *1*, 117−120.

(26) Lee, M. Y.; Hong, K. J.; Kajiuchi, T.; Yang, J. W. Synthesis of chitosan-based polymeric surfactants and their adsorption properties for heavy metals and fatty acids. *Int. J Biol. Macromol.* **2005**, *36*, 152−158.

(27) Mansoor, M. A. Pyrene fluorescence study of chitosan self-association in aqueous solution. *Carbohydr. Polym.* **1995**, *26*, 211−213.

(28) Esquenet, C.; Terech, P.; Boue, F.; Buhler, E. Structural and rheological properties of hydrophobically modified polysaccharide associative networks. *Langmuir* **2004**, *20*, 3583−3592.

Received for review September 16, 2006. Revised manuscript received March 13, 2007. Accepted March 16, 2007. This work was supported by grants from NSFC (30670566), ISTCP (2006DFA33150), and the Shandong Science Foundation (2004BS08007).

JF062648M